This article is part of the

Proceedings of the 16th Minisymposium Verfahrenstechnik and 7th Partikelforum (TU Wien, Sept. 21/22, 2020)

Title:
Downsizing and numbering-up of a fiber fractionator

Corresponding author:
Thomas Schmid (TU Graz), thomas.schmid@tugraz.at

Date of submission:
10.02.20

Date of revision:
26.08.20

Date of acceptance:
27.08.20

Chapter ID:
MoV4-(03)

Length:
4 pages

Download available from (online, open-access):
http://www.chemical-engineering.at/minisymposium

ISBN (full book):
978-3-903337-01-5

Downsizing and numbering-up of a fiber fractionator

Thomas Schmid[1,*], Stefan Radl[1]

1: Institute of Process and Particle Engineering, Graz University of Technology, Austria
* Correspondent author: thomas.schmid@tugraz.at

Keywords: cellulose fibers, hydrodynamic fractionation, mini-channel, grade efficiency

A length-based hydrodynamic fiber fractionation process has been developed as an energy efficient alternative to existing technologies (e.g., pressure screens) in order to separate short fibers from long fibers of cellulose pulp. Potential limitations to relatively low channel Reynolds numbers were resolved by a radical downsizing of the fractionation device to a channel diameter-to-fiber length ratio of $D/L_1 \leq 7$. Results of a four-step single-channel fractionator show, that placing of fractionation steps in series is the method of choice to increase fractionator capacity without affecting fractionation selectivity. For the numbering-up of fractionation channels, a novel multi-scale bifurcation distributer was designed, which was capable of (i) sufficiently splitting the feed suspension flow rate, as well as (ii) homogeneously distributing the fiber phase of the suspension. Experiments with a multi-channel fractionator prototype with eight parallel fractionation channels demonstrate the feasibility of our numbering-up strategy.

Introduction

Length-based fiber fractionation is performed to separate long fibers from short fibers and fines. The process can help to improve the energy efficiency of paper recycling [1–3], to produce high quality paper [4,5], and to produce multilayered paper [6]. State of the art fiber fractionators for this purpose are pressure screens, consisting of a screen basket and a rotor. A disadvantage of using a pressure screen for fiber fractionation is its low capacity due to its high clogging tendency, i.e., the mass ratio of fractionated fibers (or fines; accept) to fibers within the overflow (reject). One way to improve this issue is to increase the energy input by the rotor, obviously resulting in a loss of economic competitiveness.

Redlinger-Pohn et al. [7,8] have developed an energy efficient fractionation process called hydrodynamic fractionation. The process arose from the adaption of the hydrodynamic filtration process [9,10] to cellulose fibers, which consists of a flow channel with side branches: only particles having their center of mass within the branch affected volume will be sucked into the branch. These effects are also proved for free flowing cellulose fibers [11,12] and clogging issues are prevented by a backwards tilt of the branch [9]. The clue in hydrodynamic fractionation is, that it profits from network effects: for a certain range of Reynolds number *Re*, fibers suspended in a flow channel will segregate into a central plug surrounded by an almost fiber free annulus, see the *Re*-Regime *C* in Figure 1: while the pressure drop of the pulp suspension has a minimum (circles), the annulus thickness (triangles) shows a peak. The particles present in the annulus are mainly short fibers or fines. By sucking out only the annulus volume, a length-based fractionation occurs. A disadvantage of this kind of hydrodynamic fractionation is its *Re*- limitation, i.e., Redlinger-Pohn et al. [7] suggest $Re_{opt} \approx$ 1,300, which results in a limitation of consistency, i.e., $C <<$ 0.5%: For significantly lower *Re*, the annulus will decrease due to a decrease in wall lift forces caused by a decrease in shear rate; for significantly higher *Re*, the annulus will also decrease due to an increase of shear rate, which will cause the fiber plug to blur and disperse all over the channel cross section. Above described behavior has been detected for industrially relevant sized ducts; in small diameter channels, having a ratio of channel diameter to length weighted average fiber length of $D/L_1 \leq 7$, the pressure drop of a pulp suspension behaves similar to the pressure drop of pure water [13,14], see Figure 2: an extruded single-floc is formed, which is surrounded by a very thin annular lubrication layer. A dispersion of this floc in radial direction is, due to its compression, impossible.

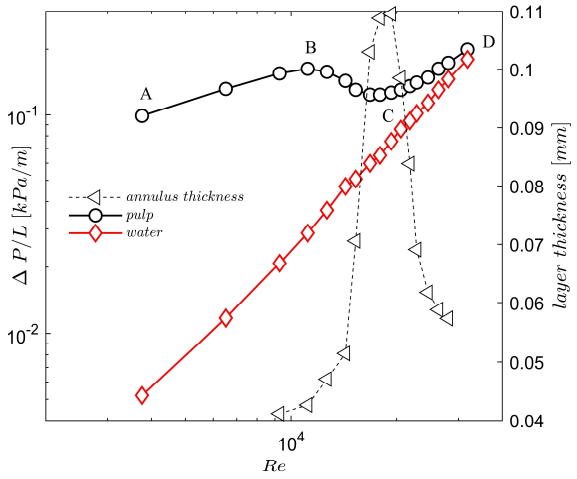

Figure 1: Pressure drop of pure water (red diamonds) and a birch fiber suspension (black circles) flow in a pipe in plug flow regime, D = 0.04m, consistency C = 1.0%, including measured annulus thicknesses, data published by Jäsberg [16].

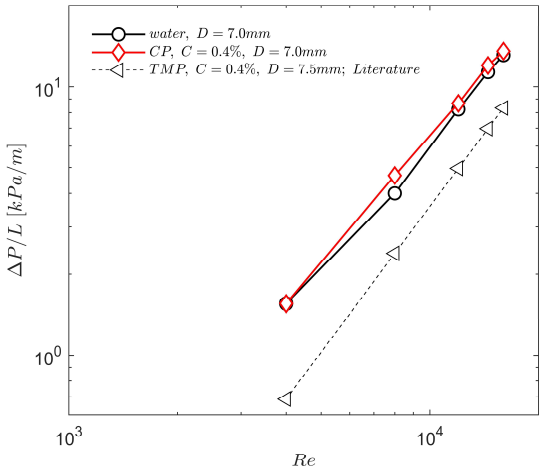

Figure 2: Pressure drop within the experimental setup (entrance channel D = 7 mm, 400 mm long + fractionator geometry) of the chemical pulp (D/L1 = 3.15), C =0.4% and pure water compared to the pressure drop of a TMP pulp in a D = 7.5 mm pipe (D/L1 = 3.18) [13].

Schmid et al. [15] have exploited this behavior by downscaling the fractionator channel to D_i = 7mm and increasing the Reynolds number to $Re >$ 10,000 to keep the suspension flowing, even at consistencies of $C >$ 0.5%. They show, that the fractionation efficiency with this novel fractionator design is independent of the Reynolds number to

a first approximation, up to at least *Re* = 25,500 and that the selectivity of the fractionation profits from high consistencies (C > 0.5%). Additionally, the fractionator design is changed to a circumferentially uninterrupted suction slot, i.e., the maximum available slot length is created.

The numbering-up of downsized fractionation channels brings one further advantage: by decreasing the channel width, the ratio between slot affected area (represented by overall channel circumference) and overall channel cross section increases, i.e., the overall size of the future fractionator decreases. Since the capacity of one fractionation step is kept relatively low to keep the fractionator selectivity high [15], also a placing of fractionator steps in series must be considered. In the following, we will present (i) the placing in series of the fractionation steps, as well as (ii) the numbering-up of the fractionation channels, both performed independently and on a lab-scale.

Experimental

The experimental setup for placing in series of fractionation steps is shown in Figure 3: the fiber suspension enters the fractionation section from a stirred tank; the driving force for flow is adjusted by (i) geodetic height of the stirred tank and (ii) by a diaphragm valve downstream the fractionator section. The fractionator section consists of four fractionators in series, and is shown in form of a sectional view of the CAD drawing. The reject of the fractionator enters a feed/reject tank to be metered by a peristaltic pump into the stirred tank again. The accept flows exit the fractionator sections via the annular side channels and are metered by a laboratory peristaltic pump, which is equipped with two pumpheads driven by the same shaft. Pumphead one meters the cumulated accept flows of the first and the second fractionator step into an accept tank. Accept three and four are metered by the second pumphead. The equal collection of two combined accept flows, i.e., to ensure, that $\dot{V}_{accept,1} = \dot{V}_{accept,2}$, turned out to be a challenge: since the total accept flow rates are very small, i.e., 50 ml/min < $\dot{V}_{accept}$ < 200 ml/min, the pressure drop within each accept channel is small compared to the pressure drop of the main channel between two steps. As a result, the four accept hoses before the T-junctions are chosen to be long (L = 1 m) and narrow (D_i = 1.6 mm) to make the main channel pressure drop marginal compared to the accept channel pressure drop.

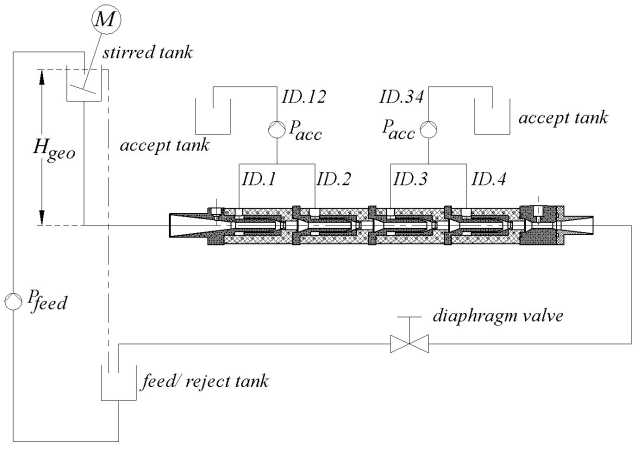

Figure 3: process diagram of the single-channel and four-step experimental setup including (i) a view of the fractionator itself, (ii) the pulp tanks for accept, feed/reject and for adjusting geodetic height upstream the fractionator, and (iii) the accept and feed pumps, both peristaltic pumps to exactly adjust flow rates.

For the numbering-up of flow channels a higher constructive effort was needed. First, a sufficient flow distributor had to be designed. There are two state of the art flow distributors for fiber suspensions: (i) the crossflow distributor and (ii) the central distributor. First experiments with a simplified lab-scale crossflow distributor, i.e., a T-junction, showed, that the distributor behaves similar to a hydrodynamic fractionator: if the flow rate into the side channel was adjusted smaller than the flow rate downstream the side channel, the downstream flow was thickened. The reason for that behavior is the radial consistency profile within the channel. Another disadvantage of a crossflow distributor would be the implementation of a recirculation pump and a control strategy thereof. Central distributors consist of a cylinder with radially distributed outlets within the cylinder wall. The suspension enters the cylinder at its bottom through a diffuser plate, its top is closed and can be eventually pressurized. This concept is rather simple, and is already applied on a lab-scale. However, the distribution to a great number of mini-channels (e.g., more than 50) would require a large diameter of the central distributor, which would lead to a comparably small velocity within the cylinder.

Since both traditional distributor concepts seem to fail for our application, we decided to develop a novel, multi-scale flow distributor, inspired by micro-reactor technology [17–19]: our novel suspension distributor consists of a bifurcation manifold, which can be combined with an upstream central distributor or crossflow distributor. The bifurcation manifold has several features: (i) each manifold includes a step diffuser to disperse fiber flocs, (ii) the flow is accelerated downstream the diffuser to generate an extensional flow, i.e., to prevent fibers from re-flocculation and (iii) the step-wise decrease in diameter offers a specific adjustment of *Re* to prevent the channels from clogging. Additive manufacturing (AM) offers the possibility to rapidly manufacture such a complex geometry in a short time and for low cost. The manufacturing process benefits from small sized parts to be coherent to our design strategy.

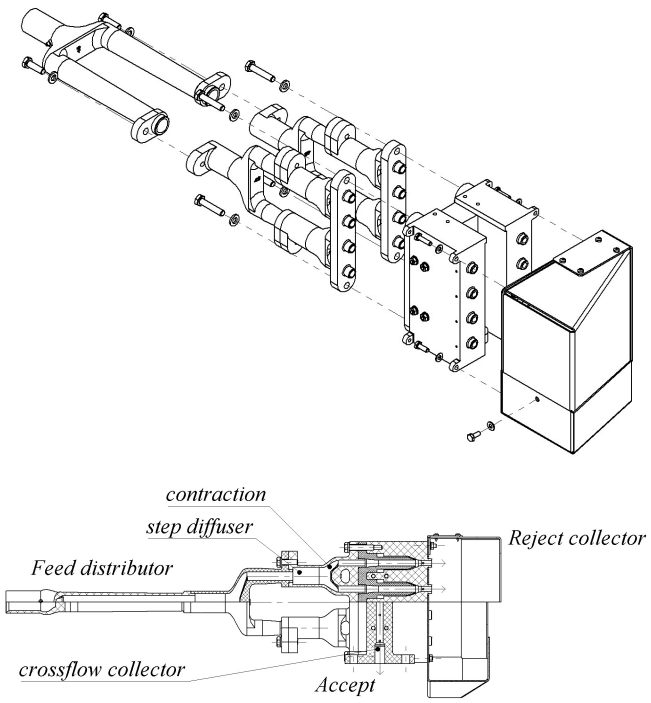

Figure 4: prototype of a multi-channel fractionator including (i) a feed pulp distributor, (ii) the fractionation section including an accept collector and (iii) a reject collector (free jet into a sheet metal box).

The first multi-channel prototype in form of an eight-channel fractionator is shown in Figure 4: the fiber suspension enters

the fractionator channels via a three-scale bifurcation distributor, the accept streams are collected by a crossflow collector, which is connected to an accept pump (laboratory syringe pump); the reject exits the fractionator in form of a free-jet and is collected by a deflector box (reject collector).

In order to evaluate the flow distribution, an adapter plate was manufactured, which contained eight hose connectors. The hoses were chosen to be one inch in diameter to keep the free-jet condition at the fractionators outlet. Each hose was then connected to a separate container, and the volumetric flow rate of each reject stream could be measured.

The evaluation of (i) capacity and (ii) selectivity of the fractionation process is performed based on grade efficiency curves. Therefore, the mass flow rates of fibers are evaluated gravimetrically, i.e., by measuring the volumetric flow rates of feed and accepts and weighing the dry mass of fibers within a sample of feed and accept. The volume weighted cumulative length distributions of fibers within the samples are evaluated by a flow-optical fiber tester by Lorentzen and Wettre, measuring projected length and width of each detected fiber, assuming each fiber to be a cylinder with constant density. The grade efficiency is then

$$T(L_{fiber}) = 1 - \frac{\dot{V}_{accept} C_{accept} \Delta Q_{accept}\left(L_{fiber}\right)}{\dot{V}_{feed} C_{feed} \Delta Q_{feed}\left(L_{fiber}\right)} \qquad (1)$$

with the volumetric flow rates of feed $\dot{V}_{feed}$ and accept $\dot{V}_{accept}$, its gravimetrically determined consistencies $C_{feed,accept}$ and the cumulative length distributions $\Delta Q_{accept,feed}$.

Results and Discussion

In a first multi-step experiment, only two fractionation steps were applied, each step equipped with a separate pump head. The accept ratio, i.e., the ratio between volumetric flow rate of the accept and volumetric flow rate of the feed, Φ^+, was adjusted to $\Phi^+ = 0.012$ for each step to realize an overall accept ratio of $\Phi^+ = 0.024$. Since the accept ratio is chosen to be comparably small, the Reynolds number within the main channel changed only marginally: it was adjusted to approx. Re = 15,750 and the feed consistency was C = 0.5%. The grade efficiency curves for this first experiment are shown in Figure 5, ID37: the grade efficiency curves of each of the two steps, i.e., ID37.1 (open circles) and ID37.2 (filled diamonds) match to a first approximation. The accumulated grade efficiency of the two-step fractionator, ID37 (open triangles), is characterized by a significant increase in capacity, i.e., for example, based on the amount of fractionated fibers within the smallest fiber class (i.e., 0 < l_{fiber} < 200 µm), the capacity doubled from approx.0.5% to approx. 1.0%. The selectivity of the process, which is characterized by the ratio between the amount of fractionated short fibers to fractionated long fibers did not suffer from this placing in series, taking a fiber length of e.g. l_{fiber} = 1.0 mm as a criterion.

In a second step, all four fractionators are connected as indicated in Figure 3: the accept streams ID56.1 and ID56.2 are combined (ID56.12) and metered by the first pumphead and the accept streams ID56.3 and ID56.4 are both metered by a second pumphead (ID56.34). The channel Reynolds number is kept similar to ID37 at approx. Re = 14,000 and the accept ratio of each pumphead is adjusted to approx. Φ^+ = 0.025, i.e., a similar value as in the previous two-step experiment. The grade efficiency curves for ID56.12 (filled triangles) as well as for ID56.34 (open rectangles) match reasonably well. Furthermore, these two curves also match the cumulated two-step curve of the previous experiment (ID37, open triangles), where the single accept flow rates could be adjusted individually to balance them. As a result, this is an indicator, that the individual accept streams in ID56.12 and ID56.34 were also evenly balanced. The capacity of ID56 (1.5%) equals the sum of the capacities of ID56.12 (0.7%) and ID56.34 (0.8%). Since the selectivity of the ID56.34 does not significantly differ from ID56.12, we cannot identify a decrease in selectivity for the overall process.

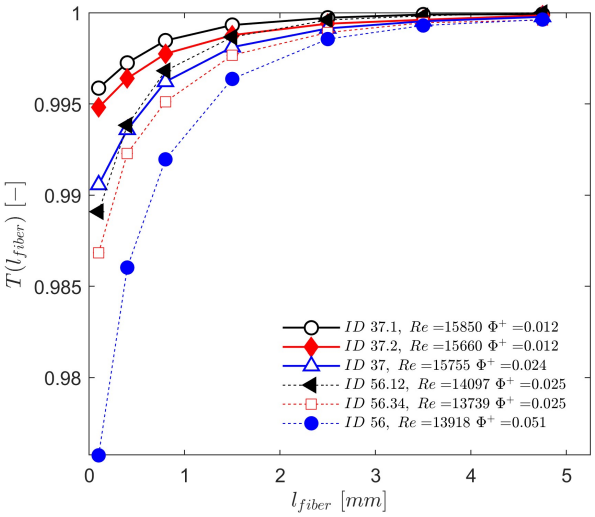

Figure 5: grade efficiency curve of (i) a single-channel two-step experiment (ID37) including the grade efficiency curves for each step (ID37.1 and ID37.2) with a feed consistency of C = 0.6% and (ii) grade efficiency curve of a single-channel four-step experiment (ID56) including the grade efficiency curves of steps one and two (ID56.12) and of steps three and four (ID56.34) with a feed consistency of C = 0.5%.

Figure 6 shows the flow rates and consistencies of the reject streams exiting the eight-channel fractionator. The flow rates vary between 4.5 l/min < $\dot{V}_{reject}$ < 5.5 l/min, which implies a channel Reynolds number of 13,600 < Re < 16,700. This Re-variation is tolerable, because the mini-channel process is not a strong function of the Reynolds number. The flow rate through each channel was in a way sufficient, since no clogging occurred. The consistency distribution varied between 0.37% < C < 0.44%, i.e., the consistency distributed sufficiently homogeneous over the distributer branches (standard deviation: 2%)

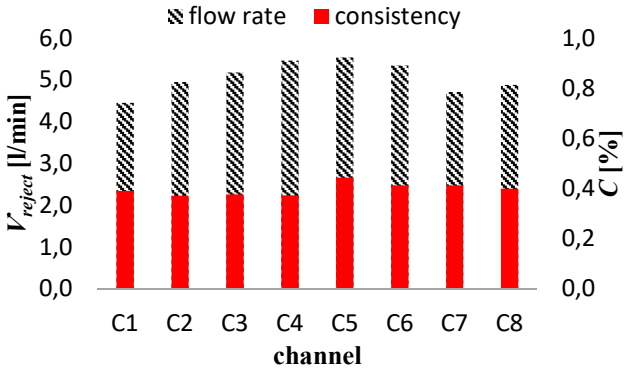

Figure 6: Reject flow rate measurement and consistency distribution over all eight fractionation channels of the eight-channel fractionator.

The fractionation efficiency of the eight-channel fractionator is compared to a single channel experiment, in order to prove our numbering-up concept, see Figure 7: the grade efficiency curves of the numbered-up experiment (ID 80) and the single channel experiment (ID73) collapse to a first approximation. Both experiments were performed at similar process conditions, i.e., an (averaged) Reynolds number of Re ≈ 15,000, an overall accept ratio of Φ^+ = 0.02 and a feed

consistency of C = 0.5%. The multi-channel experiment appears to be slightly more selective, because it has a lower long fiber acceptance, indicated by the smaller curve offset ω from T = 1 in the region of long fibers (c.f. detail in Figure 7).

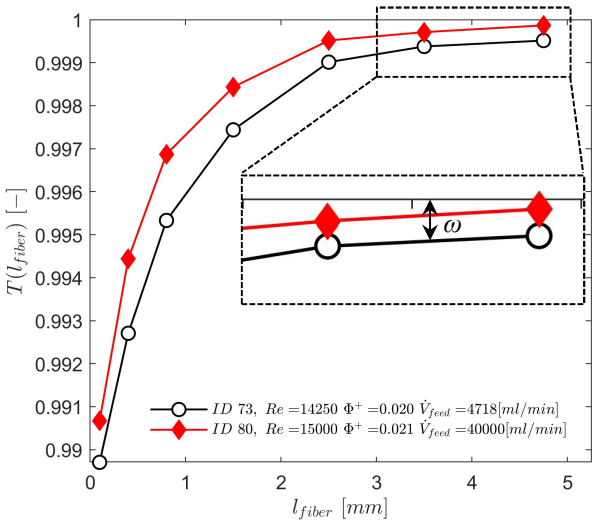

Figure 7: Grade efficiency curve of (i) a single-channel single-step experiment (ID73) and (ii) of an eight-channel single-step experiment (ID80) at both a channel Reynolds number of approx. Re = 15,000, a volumetric accept ratio of Φ^+ = 0.02 and an inlet consistency of both C = 0.5%.

Conclusions

The downsizing of the hydrodynamic fractionation device offers an efficient and coherent numbering-up strategy, since (i) the process is insensitive to varying Reynolds number within the fractionator channel, (ii) the required number of fractionation channels in parallel can be minimized, since the Reynolds number can be large in each channel and (iii), as a result, the overall size of the fractionation device can be kept small. The selectivity of the process is restricted by a low accept ratio, which limits fractionation capacity per step. We show, that placing of fractionator steps in series enables an increase of fractionation capacity while keeping fractionation selectivity relatively constant.

The numbering-up of fractionation channels is designed in a way, that all accept streams of one step are collected to a combined accept stream, which can then be more easily controlled. We show, that the collection of accept streams has no effect on fractionation. The small scale of the fractionator channels necessitates the design of a novel distributor for fiber suspensions, consisting of (i) a dispersion step, (ii) an acceleration step and (iii) a smooth forward bifurcation. Preliminary experiments show, that (i) the distribution of suspension flow rates is (due to the *Re*- independency of the process) acceptable and that (ii) the distribution of the fiber phase is sufficiently homogeneous.

All in all, we prove, that a numbering-up of our downsized mini-channel fractionator is feasible. Future studies will deal with the implementation of the design into a pilot-scale fractionation plant utilizing a multi-channel multi-step fractionator.

Acknowledgments

We gratefully acknowledge the industrial partners Sappi Austria Produktions-GmbH & Co KG, Zellstoff Pöls AG and Mondi Frantschach GmbH, and the Competence Centers for Excellent Technologies (COMET), promoted by BMVIT, BMDW, Styria and Carinthia and managed by FFG, for their financial support of the K-project FLIPPR² (Future Lignin and Pulp Processing Research – PROCESS INTEGRATION).

References

[1] A. Bjärestrand, H. Vomhoff, Upgrading Recycled Pulp Quality by Fractionation and Selective Refining, Int. Pap. IPW. 12 (2016) 40–44.

[2] H. Kraschowetz, E. Hertl, H.J. Aregger, Fractionation in DIP - Lines-A further step in waste paper recycling, Appita Annu. Conf. Exhib. 62 (2008) 177–183.

[3] K.J. Kramer, E. Masanet, T. Xu, E. Worrell, Energy Efficiency Improvement and Cost Saving Opportunities for the Pulp and Paper Industry: An ENERGY STAR Guide for Energy and Plant Managers, (2009) 176.

[4] C. Sandberg, L. Nilsson, A. Nikko, Fibre fractionation - a way to improve paper quality, in: Proc. Int. Mech. Pulping Conf., Stockholm, 1997: pp. 167–171.

[5] Y. V. Sood, P.C. Pande, S. Tyagi, I. Payra, N. Kulkarni, A.G. Kulkarni, Quality improvement of paper from bamboo and hardwood furnish through fiber fractionation, J. Sci. Ind. Res. (India). 64 (2005) 299–305.

[6] G.M. Scott, S. Abubakr, Fractionation of Secondary Fiber - A Review, Prog. Pap. Recycl. 3 (1994) 50–59.

[7] J.D. Redlinger-Pohn, W. Bauer, S. Radl, Fractionation of fibre pulp in a hydrodynamic fractionation device: influence of reynolds number and accept flow rate, Trans. 16Th Fundam. Res. Symp. Held Oxford Sept. 2017. (2017) 209–228.

[8] J.D. Redlinger-Pohn, J. König, S. Radl, Length-selective separation of cellulose fibres by hydrodynamic fractionation, Chem. Eng. Res. Des. 126 (2017) 54–66.

[9] A. Tamura, S. Sugaya, M. Yamada, M. Seki, Tilted-Branch Hydrodynamic Filtration for Length-Dependent Sorting of Rod-Like Particles, 15th Int. Conf. Miniaturized Syst. Chem. Life Sci. (2011) 1343–1345.

[10] M. Yamada, M. Seki, Hydrodynamic filtration for on-chip particle concentration and classification utilizing microfluidics, Lab Chip. 5 (2005) 1233.

[11] J.A. Olson, The Effect of Fibre Length on Passage Through Narrow Apertures, University of British Columbia, 1996.

[12] A. Kumar, Passage of Fibres Through Screen Apertures, University of British Columbia, 1991.

[13] G.G. Duffy, L. Abdullah, Fibre suspension flow in small diameter pipes, Appita J. 56 (2003) 290–295.

[14] G.G. Duffy, S. Ramachandra, Validation of flow mechanisms of fibre suspensions in small diameter pipes, Appita J. 58 (2005) 374–377.

[15] T.J.R. Schmid, J.D. Redlinger-Pohn, S. Radl, Length-based hydrodynamic fractionation of highly networked fibers in a mini-channel, (2019), manuscript submitted to the Nordic Pulp&Paper Research Journal.

[16] A. Jäsberg, Flow Behaviour of Fibre Suspension in Straight Pipes: New Experimental Techniques and Multiphase Modeling, University of Jyväskylä, 2007.

[17] M. Saber, J.M. Commenge, L. Falk, Rapid design of channel multi-scale networks with minimum flow maldistribution, Chem. Eng. Process. Process Intensif. 48 (2009) 723–733.

[18] M. Saber, J.M. Commenge, L. Falk, Microreactor numbering-up in multi-scale networks for industrial-scale applications: Impact of flow maldistribution on the reactor performances, Chem. Eng. Sci. 65 (2010) 372–379.

[19] J.M. Commenge, M. Saber, L. Falk, Methodology for multi-scale design of isothermal laminar flow networks, Chem. Eng. J. 173 (2011) 334–340.